

# SPECT/CT\*

Andreas K. Buck<sup>1</sup>, Stephan Nekolla<sup>1</sup>, Sibylle Ziegler<sup>1</sup>, Ambros Beer<sup>1</sup>, Bernd J. Krause<sup>1</sup>, Ken Herrmann<sup>1</sup>, Klemens Scheidhauer<sup>1</sup>, Hans-Juergen Wester<sup>1</sup>, Ernst J. Rummeny<sup>2</sup>, Markus Schwaiger<sup>1</sup>, and Alexander Drzezga<sup>1</sup>

<sup>1</sup>Department of Nuclear Medicine, Technische Universität München, München, Germany; and <sup>2</sup>Department of Radiology, Technische Universität München, München, Germany

In view of the commercial success of integrated PET/CT scanners, there is an increasing interest in comparable SPECT/CT systems. SPECT in combination with CT enables a direct correlation of anatomic information and functional information, resulting in better localization and definition of scintigraphic findings. Besides anatomic referencing, the added value of CT coregistration is based on the attenuation correction capabilities of CT. The number of clinical studies is limited, but pilot studies have indicated a higher specificity and a significant reduction in indeterminate findings. The superiority of SPECT/CT over planar imaging or SPECT has been demonstrated in bone scintigraphy, somatostatin receptor scintigraphy, parathyroid scintigraphy, and adrenal gland scintigraphy. Also, rates of detection of sentinel nodes by biopsy can be increased with SPECT/CT. This review highlights recent technical developments in integrated SPECT/CT systems and summarizes the current literature on potential clinical uses and future directions for SPECT/CT in cardiac, neurologic, and oncologic applications.

**Key Words:** scintigraphy; SPECT; CT; PET; hybrid imaging

**J Nucl Med 2008; 49:1305–1319**

DOI: 10.2967/jnumed.107.050195

**H**ybrid imaging techniques allow the direct fusion of morphologic information and functional information. Since its introduction to clinical medicine in 2001, PET/CT has become the fastest growing imaging modality (1,2). CT coregistration has led to definite diagnoses by PET and more acceptance of functional imaging. Recently, integrated SPECT/CT scanners have been made available. With SPECT/CT, lesions visualized by functional imaging can be correlated with anatomic structures. The addition of anatomic information increases the sensitivity as well as the specificity of scintigraphic findings (Fig. 1). SPECT/CT has an additional value in sentinel lymph node (SLN) mapping,

especially in head and neck tumors and tumors draining into pelvic nodes. In addition to improved anatomic localization of scintigraphic findings, SPECT/CT offers the opportunity to add true diagnostic information derived from CT imaging. Given the growing number of studies demonstrating the added value of hybrid SPECT/CT relative to single imaging modalities, it appears likely that this promising technique will play an increasingly important role in clinical practice. The broad spectrum of existing SPECT tracers and their widespread availability suggest that SPECT/CT can be complementary to PET/CT.

## TECHNICAL ASPECTS OF SPECT/CT

Before the introduction of dedicated SPECT/CT cameras, various software algorithms were established to allow image fusion for anatomic imaging (CT or MRI) and functional imaging (SPECT) (3). In the early 1980s, efforts were made to allow image fusion in brain studies. Current software algorithms permit highly accurate coregistration of anatomic and functional datasets. This kind of nonrigid image coregistration is therefore a regular component in daily clinical practice, such as image-guided surgery or radiation treatment planning. However, motion artifacts markedly affect image fusion in the thorax, abdomen, pelvis, or head and neck region when CT and SPECT acquisitions are obtained separately (4,5). Functional images of the thorax or the abdomen contain little or no anatomic landmarks that can be correlated with anatomic reference points. Moreover, the chest and the abdomen do not represent rigid structures. Differences in patient positioning and respiratory motion make the correct alignment of anatomic and functional images even more complicated. More recently, 3-dimensional elastic transformations or nonlinear warping has been established to further improve the accuracy of image fusion. With these modern approaches, the accuracy of software-based image coregistration is in the range of approximately 5–7 mm (6). Although software algorithms are not in widespread clinical use for image coregistration of the abdomen or the thorax, this technology will still play an important role by allowing the correction of misregistrations attributable to patient motion or breathing artifacts, which may also arise from integrated SPECT/CT cameras.

Received Mar. 26, 2008; revision accepted Jun. 20, 2008.

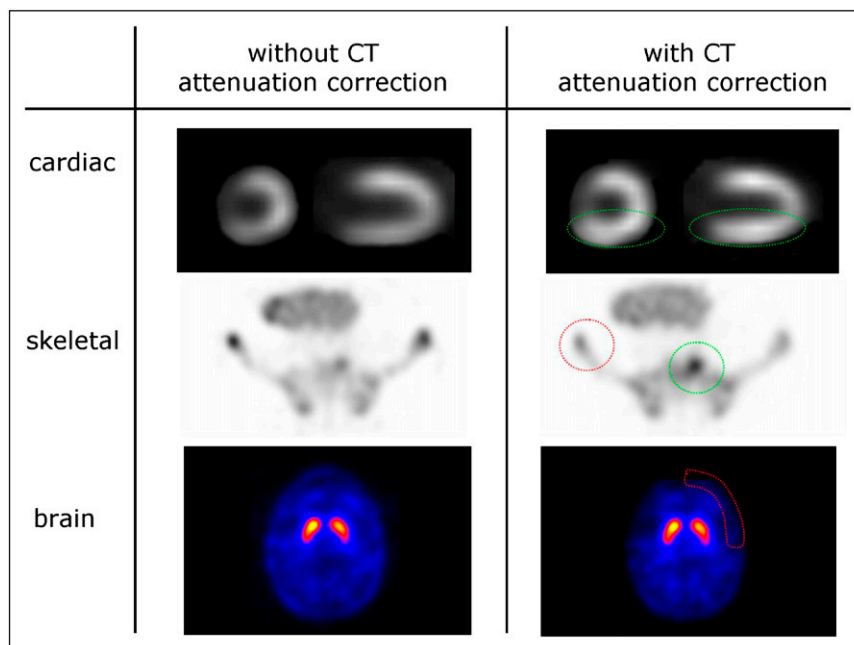
For correspondence or reprints contact: Andreas K. Buck, Department of Nuclear Medicine, Technische Universität München, Ismaninger Strasse 22, D-81675 Munich, Germany.

E-mail: andreas.buck@tum.de

\*NOTE: FOR CE CREDIT, YOU CAN ACCESS THIS ACTIVITY THROUGH THE SNM WEB SITE ([http://www.snm.org/ce\\_online](http://www.snm.org/ce_online)) THROUGH AUGUST 2009.

No potential conflict of interest relevant to this article was reported. COPYRIGHT © 2008 by the Society of Nuclear Medicine, Inc.

**FIGURE 1.** Impact of CT attenuation correction. Upper row (myocardial perfusion scintigraphy) shows attenuation of  $^{99m}\text{Tc}$ -MIBI uptake in inferior myocardium. CT-corrected image demonstrates normal perfusion of inferior myocardium (green circles). Middle row (skeletal scintigraphy with  $^{99m}\text{Tc}$ -hydroxymethylene diphosphonate) shows superior localization of bone metastasis in os sacrum (green circle) after CT attenuation correction. Lower row shows CT attenuation correction of brain study ( $^{99m}\text{Tc}$ -iodobenzamide SPECT). Without CT attenuation correction, background activity may be overestimated, especially in peripheral structures (red circles) and may appear with similar intensity as pathologic findings (e.g., skeletal scintigraphy, middle row).



Initial work was done by Hasegawa et al., who introduced a system that is capable of simultaneous CT and SPECT acquisitions (7). This group was the first to demonstrate that CT data can be used for attenuation correction, allowing superior quantification of radiotracer uptake. This technology translated into the first commercial SPECT/CT system, Hawkeye, which was introduced by GE Healthcare (8). Here, the modalities are combined, allowing sequential CT and SPECT acquisitions with only an axial shift of the patient between measurements. An enhanced version developed by GE Healthcare contained a 4-row multidetector CT capable of acquiring four 5-mm slices instead of one 10-mm slice. Philips combined a 6- or 16-slice CT scanner with a Skylight double-head camera system (Precedence). Philips also introduced a system for scientific purposes combining SPECT with 64-slice CT. Siemens Medical Solutions combined an E-Cam dual-detector  $\gamma$ -camera system with optional 1-, 2-, or 6-slice CT. With both systems, slice thickness can be adjusted from 0.6 to 10 mm, and the scan speed is  $<30$  s for a 40-cm axial field of view. With the availability of coregistered CT information for the patient, methods that include spatially dependent collimator deblurring become feasible (9). Algorithms that combine this approach with attenuation on scatter correction (both based on CT information) have been implemented in SPECT/CT systems and may enable quantitative SPECT (10).

#### SUGGESTED PROTOCOLS FOR SPECT/CT

Although planar imaging and SPECT are routinely performed studies and respective protocols have been documented for various clinical settings, the roles of CT coregistration and specific imaging protocols have not yet

been clearly defined. In general, instead of standard protocols, combined SPECT/CT procedures should be selected on an individual basis and should reflect clinical needs. The radiation dose delivered by CT is a major issue in this regard, because diagnostic CT can increase the overall radiation dose by up to 14 mSv (11). Low-dose CT is associated with relatively low radiation doses of 1–4 mSv and should be sufficient for anatomic referencing of SPECT lesions and attenuation correction (Table 1). Usually, if a recent contrast-enhanced diagnostic CT scan is available, there is no need to perform another contrast-enhanced CT scan during SPECT/CT. Also, when SPECT/CT is performed for treatment monitoring and follow-up, low-dose CT should be sufficient. Therefore, the use of low-dose, nonenhanced spiral CT can be recommended in most cases when SPECT/CT is performed for anatomic referencing or attenuation correction. The standard protocol for integrated SPECT/CT at our institution (Siemens Symbia 6) is shown in Table 1.

When SPECT/CT is performed for tumor staging or restaging, the detection of small pulmonary nodules that may be negative on functional imaging is important. Therefore, the acquisition of an additional low-dose CT scan of the thorax during maximal inspiration should be considered for patients at risk for the presence of lung metastases (Table 1). This strategy applies especially to patients who have high-risk differentiated thyroid cancer and are undergoing radioiodine scintigraphy. In this setting, an additional 40-mA low-dose CT scan acquired during inspiration is a feasible approach, because it has been demonstrated that a reduction of the tube current to 40 mA results in satisfactory image quality and reduces overall radiation exposure (11).

**TABLE 1**  
Suggested CT Protocols\* for Inclusion in Noncardiac SPECT/CT Protocols

Protocol	Parameter	Comments
SPECT-guided low-dose CT	Indications (general)	Preferred protocol when recent diagnostic CT is available and when follow-up studies are performed (monitoring of response to treatment)
	Indications (specific)	Further anatomic localization or characterization of focal pathology present on planar or SPECT images, e.g., at bone scintigraphy, <sup>131</sup> I scintigraphy (thyroid cancer), sentinel node scintigraphy, <sup>99m</sup> Tc-MIBI SPECT (parathyroid tumors), <sup>123</sup> I-MIBG SPECT (adrenocortical tumors), or <sup>111</sup> In-pentetreotide imaging (neuroendocrine tumors)
	Field of view	Including all areas with nonclassifiable scintigraphic lesions, e.g., cervical, thoracic, and abdominal regions, pelvis, skull, extremities, or any combination of these
	CT overview (topogram)	Covering field of view as indicated earlier
	CT scan (tomogram)	
	Scan direction	Caudocranial
	Tube current	20–40 mA
	Tube voltage	130 kV
	Collimation	Depending on CT scanner; thinnest possible collimation for optimal multiplanar reconstructions; in areas prone to breathing artifacts, thicker collimation may be necessary to reduce scan duration and to minimize motion artifacts
	Slice thickness	5 mm; increment of 2.5 mm; thinnest possible slice thickness with overlap in reconstruction increment necessary for optimal 3-dimensional reconstructions
	Breathing protocol (general)	Shallow breathing; breath holding in expiration when lower thorax is scanned
	Breathing protocol (screening for lung metastases)	Maximum inspiration during acquisition of CT
	Radiation dose (in addition to that of SPECT)	2–4 mSv (depending on field of view in z-axis)
	SPECT-guided diagnostic CT	Indications (general)
Indications (specific)		Further anatomic localization or characterization of lesions present at bone scintigraphy, <sup>131</sup> I scintigraphy (thyroid cancer, cervical region), <sup>99m</sup> Tc-MIBI SPECT (parathyroid tumors), <sup>123</sup> I-MIBG SPECT, or <sup>111</sup> In-pentetreotide imaging, especially when sufficient diagnostic accuracy cannot be expected from low-dose CT (e.g., when lesions are suspected in mediastinum or in proximity of liver or intestinal structures)
Field of view		Including areas with lesions present on planar or SPECT images or areas with suspected lesions (e.g., upper gastrointestinal tract for detection of pheochromocytoma)
CT overview (topogram)		Covering field of view as indicated earlier
CT scan (tomogram)		Specific protocols should be selected according to clinical needs (e.g., 3-phase CT of liver)
Scan direction		Caudocranial
Scan delay		60–80 s after start of intravenous injection of contrast material (depending on field of view in z-axis)
Tube current		100 mA
Tube voltage		130 kV
Collimation		Depending on CT scanner; thinnest possible collimation for optimal multiplanar reconstructions; in areas prone to breathing artifacts, thicker collimation may be necessary to reduce scan duration and to minimize motion artifacts
Slice thickness		5 mm; increment of 2.5 mm; thinnest possible slice thickness with overlap in reconstruction increment necessary for optimal 3-dimensional reconstructions
Breathing protocol (general)		Shallow breathing; breath holding in expiration when lower thorax is scanned
Breathing protocol (screening for lung metastases)		Breath holding in maximum inspiration during acquisition of CT
Radiation dose (in addition to that of SPECT)		6–14 mSv (depending on field of view in z-axis)

\*Performed directly before or after SPECT acquisition.

**TABLE 2**  
Suggested CT Protocols for Inclusion in Cardiac SPECT/CT Protocols

Protocol	Parameter	Comments
Low-dose cardiac CT	Indications	Coronary artery calcium (CAC) scoring; attenuation correction
	CT overview (topogram)	140–180 mm
	CT scan (tomogram)	Electrocardiographic gating mandatory for CAC scoring
	Field of view	Sternum–thoracic spine (140–180 mm)
	Acquisition	Diastolic phase
	Tube current	20–40 mA
	Tube voltage	130 kV
	Slice thickness	≤3 mm; increment of ≤3 mm
	Breathing protocol	Breath holding
	Radiation dose (in addition to that of SPECT)	1–3 mSv
Diagnostic cardiac CT (64-slice CT)	Indications	CT coronary angiography
	CT scan (tomogram)	Electrocardiographic gating mandatory
	Field of view	Sternum–thoracic spine (140–180 mm)
	Acquisition	Diastolic phase
	Scan delay	“Smart preparation” (~10 s after start of intravenous injection of contrast material [100 mL]; flow rate of 4 mL/s)
	Tube current	≤900 mA
	Tube voltage	130 kV
	Collimation	Thinnest possible collimation necessary for optimal 3-dimensional reconstructions
	Slice thickness	≤3 mm; increment of ≤3 mm; thinnest possible slice thickness with overlap in reconstruction increment necessary for optimal 3-dimensional reconstructions
	Breathing protocol	Breath holding
Radiation dose (in addition to that of SPECT)	4–14 mSv	

Compared with PET/CT, diagnostic CT protocols including intravenous or oral contrast agent enhancement are seldom performed at SPECT/CT but may be appropriate in certain clinical situations (Tables 1 and 2). These protocols will have to be implemented and modified continually, especially with the availability of new scanners offering very high spatial resolution (64-slice CT). Potential CT protocols suitable for cardiac imaging are discussed later (Table 2).

### SPECT/CT FOR SLN MAPPING

For patients with cancer, accurate lymph node staging is mandatory for appropriate treatment planning. A combination of lymphoscintigraphy before surgery and mapping with blue dye during surgery has been demonstrated to be a practicable approach for accurately localizing the SLN. Although most sentinel nodes can be identified during surgery with a hand-held probe, SLN identification may be impossible in certain cases. Localization with CT coregistration before surgery may facilitate surgical access and thus improve overall detection rates. The added value of CT coregistration for SLN mapping has been demonstrated by several groups. Although inguinal and lower axillary nodes can be reliably detected on planar scintigrams, anatomic coregistration represents a valuable tool for SLN detection in the pelvis, the mediastinum, or the

head and neck region. For patients with melanoma of the head and neck or the trunk, a pilot study indicated that SPECT/CT enabled the detection of sentinel nodes in up to 43% of patients with negative planar scintigrams (12). For patients with early-stage cervical cancer (13) and invasive bladder cancer (14), better detection of sentinel nodes by SPECT/CT than by planar scintigrams was described. The CT portion of the examination was especially helpful for the identification of SLNs during surgery. For 20 patients with head and neck cancer, Khafif et al. reported a sensitivity of SPECT/CT of 87.5% (15). SPECT/CT further improved SLN identification and localization over those provided by planar images for 6 patients (30%). For a series of 34 patients, SPECT/CT identified sentinel nodes in 94% of patients (32/34) and identified additional nodes in 15 (47%) of those 32 patients (16). More accurate localization of SLNs in oral cavity squamous cell carcinoma was described by Keski-Santti et al. (17). Superior topographic SLN identification was described in 2 further studies of head and neck cancer or melanoma (12,18).

Husarik and Steinert examined the added value of SPECT/CT in breast cancer (Fig. 2) (19). For 41 consecutive patients, findings from planar scintigrams and SPECT/CT were identical in only 7 patients (17%); SPECT/CT indicated the correct anatomic localization in 29 patients (70%), according to the American Joint Committee on Cancer staging system

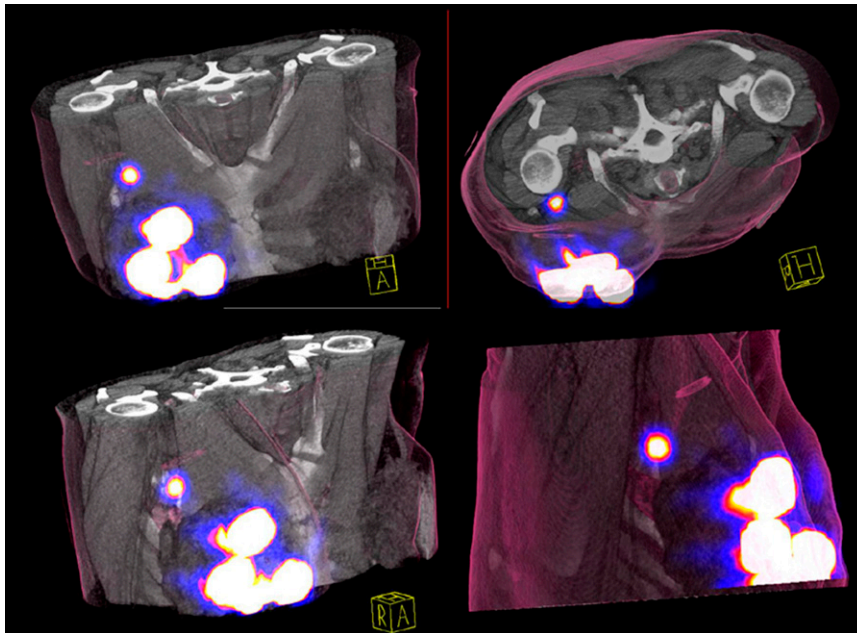


**FIGURE 2.** Accurate anatomic localization of sentinel node in patient with breast cancer by sentinel node scintigraphy ( $^{99m}\text{Tc}$ -Nanocol; Amersham) and CT coregistration. Correct anatomic localization of sentinel node in left axilla is illustrated by 3-dimensional projections of fused images.

(levels I–III). For 6 patients, additional SLNs were detected. For 26 patients (63%), exact anatomic localization could be derived exclusively from SPECT/CT; 3 sentinel nodes close to the injection site were not detected by SPECT but could be clearly visualized by SPECT/CT. Similar findings were described earlier by Lerman et al. (20). For 157 consecutive patients, 13% of sentinel nodes were visualized by SPECT/CT but not on planar scintigrams. Unexpected sites of drainage and non-node-related hot spots were identified for 33 patients. For a prospective series of 51 patients, sentinel nodes could be assigned to axillary levels I–III on the basis of SPECT/CT data but not on the basis of planar images (21). In a pilot study by van der Ploeg et al., SPECT/CT was superior to SPECT for SLN detection; for 4 of 31 patients, 6 additional SLNs were detected by SPECT/CT, leading to a change in management for 5% of patients because of upstaging in the axilla (22). SPECT/CT has been shown to be especially useful in overweight patients. In a prospective study of 220 patients with breast cancer, 122 patients had a body mass index of greater than 25 (23). For 49 patients (22%), planar images failed to identify a sentinel node. However, for 29 of these 49 patients (59%), sentinel nodes could be identified by SPECT/CT. Overall, the sensitivity of SPECT/CT in overweight patients was 89%. SPECT/CT was also superior to blue dye labeling during surgery and identified sentinel nodes in 75% of patients in whom the blue dye technique failed to detect sentinel nodes. Although the current literature does not indicate a major role for SPECT/CT in SLN identification in breast cancer, this modality may be helpful when the standard approach fails to identify the SLN.

### SPECT/CT IN SKELETAL DISEASES

For more than 30 y, planar bone scintigraphy has been used as a valuable method for sensitively detecting or character-

izing focal bone pathology; more recently, SPECT has been used in this capacity (24). Although functional bone imaging is a highly sensitive method, it lacks specificity (25). Therefore, radiography, CT, or MRI is frequently performed after bone scintigraphy to further characterize lesions evident on bone scans. Integrated SPECT/CT offers a direct correlation of focal bone pathology with anatomic structures and therefore minimizes the number of equivocal findings.

### Applications in Malignant Skeletal Diseases

Screening for bone metastases and evaluation of the treatment response are the most frequent indications for bone scanning. Although the majority of bone metastases appear as hot spots, some appear as cold lesions. Benign lesions, such as hemangioma, may also appear as cold, making the differential diagnosis problematic. The differentiation of benign and malignant lesions can usually be achieved with CT coregistration and is a major advantage of SPECT/CT (Fig. 3). In addition, fused images can be used to further guide biopsies of bone lesions.

A normal tracer distribution on planar bone scans usually makes the use of SPECT/CT unnecessary. Although in many cases the correct diagnosis can be derived from planar bone scans, SPECT/CT is necessary to make the correct diagnosis in cases of undefined lesions. In particular, scintigraphic lesions in the spine or pelvis frequently may not be defined exactly, requiring the additional use of CT or MRI. Recently, image coregistration was demonstrated to be superior to planar radiographic techniques or SPECT and proved useful in further characterizing benign skeletal abnormalities. The presence of accompanying complications, such as fractures or compression of the spinal cord, can also be diagnosed in a single examination (26).

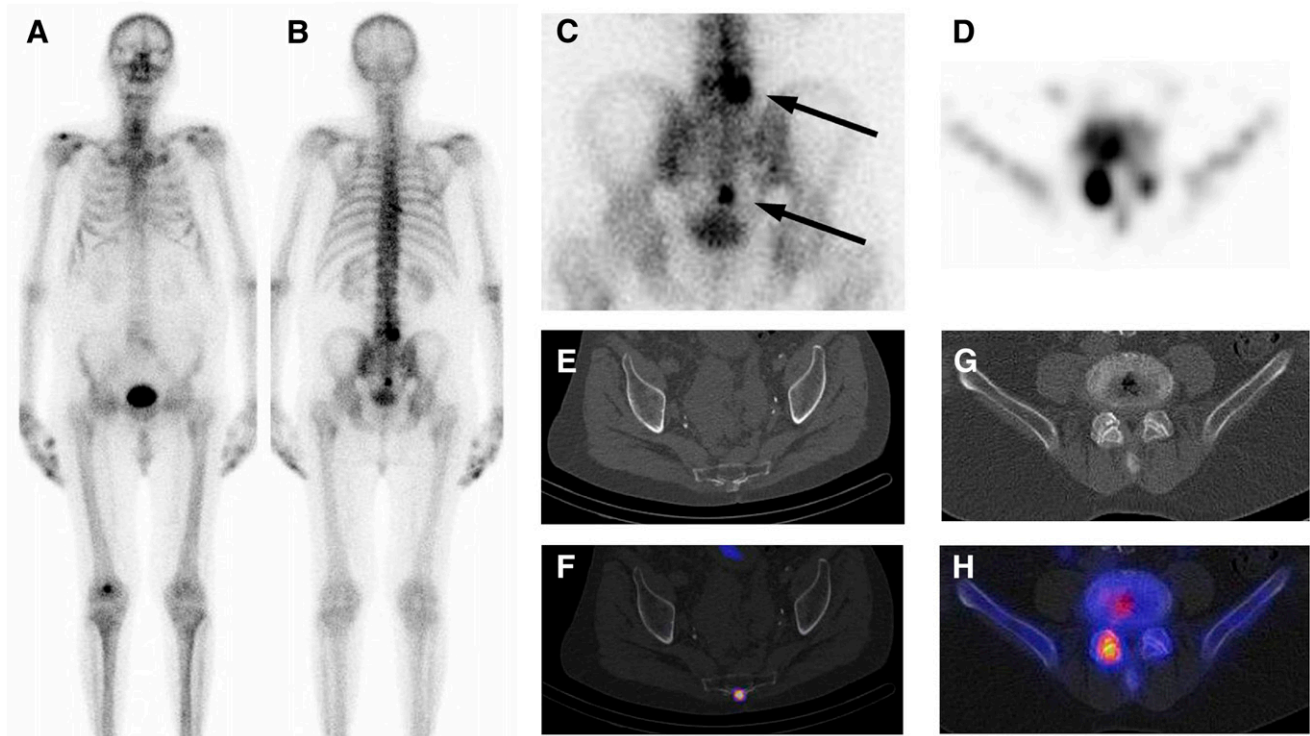


**FIGURE 3.** Patient with lung cancer and 2 hot spots, in lower lumbar spine and pelvis (os sacrum). (A and B) Planar scintigrams from skeletal scintigraphy ( $^{99m}\text{Tc}$ -hydroxymethylene diphosphonate). (C) Detailed view of pelvis with 2 hot spots (arrows). (D) Transverse section of upper lesion in lumbar vertebra 5. (E) Small osteolytic lesion with intense tracer uptake indicating bone metastasis in lower pelvis. (F) Fused image. (G and H) Spondylarthrosis of right facet joint with intense tracer uptake indicating degenerative lesion.

The first report demonstrating the superiority of SPECT/CT over planar imaging or SPECT was published by Römer et al. (27). In this retrospective study, SPECT-guided CT was reported to clarify more than 90% of bone lesions that were indeterminate at SPECT: 63% of indeterminate findings could be definitely assigned as benign lesions involving mostly osteochondrosis, spondylosis, or spondylarthrosis of the spine; 29% of lesions could be clearly assigned as osteolytic or osteosclerotic bone metastases; and 4 lesions (8%) remained indeterminate at SPECT/CT because of a missing anatomic correlate. The majority of these lesions were located in the ribs or scapula. Because the performance of MRI in the thorax is affected by motion artifacts, the authors concluded that even MRI might not be able to confirm or exclude bone metastases in such lesions. The study also indicated that exact matching of functional and anatomic data may be necessary, especially in small anatomic structures. Small osteolytic bone metastases were observed in close proximity to facet joints, potentially causing misinterpretation of lesions at SPECT. The concept of Römer et al. (27) included the use of SPECT data for determination of the field of view for CT, resulting in reduced additional radiation exposure. On a per-patient basis, the mean radiation exposure from additional CT was as low as 2.3 mSv. SPECT-guided CT therefore results in acceptable overall radiation exposure. The use of CT data for attenuation

correction may also increase the performance of SPECT, but this issue has not been studied in detail (28,29).

Using a combination of a dual-head SPECT camera and a nondiagnostic low-dose CT scanner, Horger et al. were also able to correctly classify 85% of unclear foci; in comparison, 36% of such foci were correctly classified by SPECT alone (30). Integrated SPECT/CT also seems to be superior to side-by-side reading of SPECT and CT images. Using juxtaposed CT and SPECT scanners, Utsunomiya et al. demonstrated that fused images were superior to side-by-side reading for the differentiation of malignant from benign lesions (31).

#### Applications in Benign Skeletal and Infectious Diseases

Even-Sapir et al. reported recently that SPECT/CT allowed a definite diagnosis for the majority of indeterminate scintigraphic findings in nononcologic situations (32). Infectious bone lesions, such as osteomyelitis, may be diagnosed by 3-phase bone scintigraphy with  $^{99m}\text{Tc}$ -labeled diphosphonates. This approach has high sensitivity but lacks specificity. Another option is the use of radiolabeled autologous leukocytes (WBC), still considered the gold standard for localizing an area of infection by scintigraphic procedures. A more practicable approach is the use of  $^{99m}\text{Tc}$ -labeled monoclonal antigranulocyte antibodies directed against the CD66 antigen, which is expressed on

granulocytes and macrophages.  $^{99m}\text{Tc}$ -labeled ciprofloxacin was recently suggested to specifically detect infection through the accumulation of the radiotracer in living bacteria. CT coregistration may improve the specificity as well as the sensitivity of these scintigraphic techniques. CT is able to detect small areas of cortical destruction and to identify soft-tissue abscesses or empyema located in neighboring soft-tissue structures. CT data can be correlated with the accumulation of granulocytes or increased bone turnover, as indicated by scintigraphy, thus confirming or excluding infectious bone lesions. It is obvious that combined imaging makes the interpretation of SPECT and CT easier and more reliable.

The added value of SPECT/CT for diagnosing infections has been demonstrated by several authors (33–40). Bar-Shalom et al. recently evaluated the role of SPECT/CT in the diagnosis and localization of infections by using  $^{67}\text{Ga}$ - or  $^{111}\text{In}$ -labeled WBC (33). The patients examined had fever of unknown origin and suspected osteomyelitis, soft-tissue infection, or vascular graft infection. SPECT/CT provided additional information for the diagnosis and localization of infections in 48% of patients (39/82). For 4 patients with physiologic bowel uptake, SPECT/CT allowed the exclusion of infection, and the diagnosis based on SPECT/CT was incorrect in 2 other patients. The authors concluded that SPECT/CT with  $^{67}\text{Ga}$ - or  $^{111}\text{In}$ -labeled WBC made an incremental contribution to scintigraphy by improving the diagnosis, localization, or definition of the extent of disease. Another study evaluated the performance of SPECT/CT in 28 patients with suspected bone infection or infection of orthopedic implants. WBC planar scanning or SPECT accurately detected infections in 18 of 28 patients, with true-negative results in 10 of 28 patients; SPECT/CT provided accurate anatomic localization for all lesions. There was a significant clinical contribution of SPECT/CT in 36% of patients. For

patients with osteomyelitis, SPECT/CT was also able to differentiate soft-tissue from bone involvement and allowed the correct diagnosis of osteomyelitis in patients with structural tissue alterations attributable to trauma. The superiority of SPECT/CT with  $^{111}\text{In}$ -labeled WBC over side-by-side reading of SPECT and CT images was also suggested by a recent pilot study (36).

The added value of integrated SPECT/CT relative to triple-phase bone scintigraphy was evaluated by Horger et al. (35). For 31 patients with pathologic results from a triple-phase bone scan, the sensitivity and the specificity of SPECT/CT were 78% and 86%; those of SPECT and planar imaging were 78% and 50%, respectively. However, a combination of SPECT and separately performed MRI, radiography, or CT returned the highest sensitivity. SPECT/CT avoided false-positive findings and reduced the number of equivocal findings, but an additional benefit beyond the benefits of separately performed imaging modalities has not been demonstrated.

### SPECT/CT IN DIFFERENTIATED THYROID CANCER

In patients with differentiated thyroid carcinoma, whole-body imaging after oral administration of  $^{131}\text{I}$  or  $^{123}\text{I}$  is commonly performed to identify residual or metastatic disease.  $^{131}\text{I}$  scintigraphy has a higher sensitivity than morphologically based imaging modalities. However, the interpretation of  $^{131}\text{I}$  images may be difficult because of the absence of anatomic landmarks. Therefore, precise localization of hot spots is frequently not possible. In addition, physiologic uptake of  $^{131}\text{I}$  may cause false-positive findings (Fig. 4). Integrated SPECT/CT potentially allows the differentiation of physiologic, artificial, and pathologic uptake of  $^{131}\text{I}$  (41). In a retrospective study by Tharp et al., SPECT/CT had an incremental diagnostic value for 41 of 71 patients

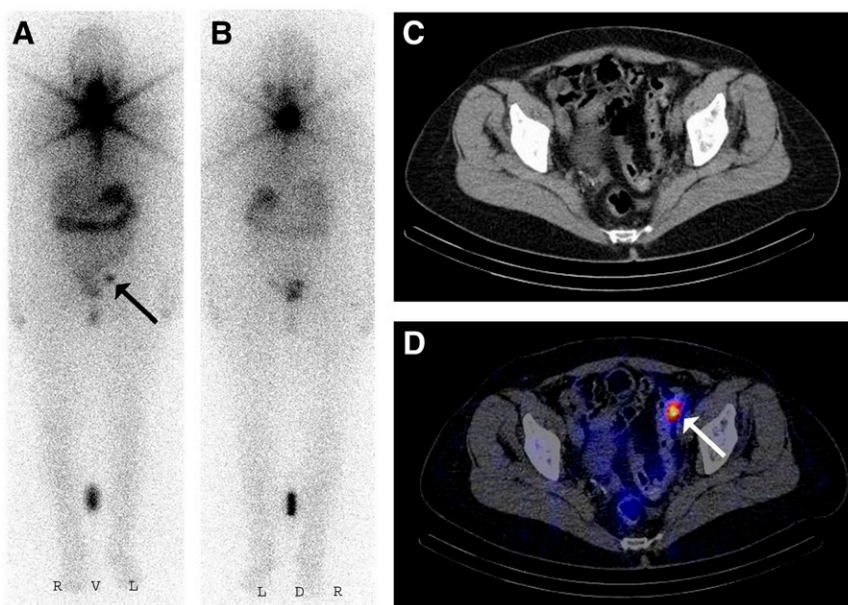


**FIGURE 4.** Exact delineation of focal pelvic  $^{131}\text{I}$  uptake in patient with differentiated thyroid cancer. (A and B) Planar  $^{131}\text{I}$  scintigrams (anterior view [A] and posterior view [B]) showing focal tracer uptake in left pelvic region (arrow). Lesion cannot be definitely assigned as benign or solitary bone metastasis. (C and D) Corresponding CT section (C) and fused SPECT/CT image (D) demonstrating non-specific tracer uptake in diverticulum of colon (arrow).

(58%) (42). In particular, in the neck region, SPECT/CT allowed the precise characterization of equivocal lesions for 14 of 17 patients and changed the lesion location for 5 patients. SPECT/CT also improved the characterization of indeterminate findings as definitely benign in 13% of patients (9/71) and the precise assignment of metastases to the skeleton in 17% of patients (12/71) and to the lungs versus the mediastinum in 7% of patients (5/71). SPECT/CT further optimized the assignment of  $^{131}\text{I}$  uptake to lymph node metastases versus remnant thyroid tissue and to lung versus mediastinal metastases. Overall, additional findings at SPECT/CT had an impact on management for 41% of patients.

In a study by Yamamoto et al. of 17 patients with differentiated thyroid carcinoma, fusion of SPECT and CT images with external markers improved the diagnosis in 15 of 17 patients (88%), mainly because of better anatomic localization of scintigraphic findings and differentiation of physiologic from specific uptake (43). Fused images resulted in a change in management for 4 of 17 patients (24%). A pilot study of 25 patients undergoing ablative radioiodine treatment of the thyroid also indicated an added value of SPECT/CT image fusion. Using an integrated SPECT/CT camera, Ruf et al. reported superior anatomic localization of 44% of suspected lesions (17/39) (44). The findings returned by fused images influenced therapeutic management for 25% of patients (6/24).

### SPECT/CT IN PARATHYROID TUMORS

In primary hyperparathyroidism,  $^{99\text{m}}\text{Tc}$ -methoxyisobutylisonitrile (MIBI) scintigraphy plays a minor role, because bilateral neck exploration has a success rate of up to 95%. However, with the increasing use of minimal invasive parathyroidectomy, presurgical imaging and precise localization of a parathyroid adenoma are critical for successful surgery. For a series of 110 patients, Lavelly et al. compared the diagnostic performance of planar imaging, SPECT,

SPECT/CT, and single- and dual-phase  $^{99\text{m}}\text{Tc}$ -MIBI parathyroid scintigraphy (45). In this prospective study, dual-phase planar imaging, SPECT, and SPECT/CT were significantly more accurate than single-phase early or delayed planar imaging. Early-phase SPECT/CT in combination with any delayed imaging method (planar or SPECT) was superior to dual-phase planar imaging or dual-phase SPECT with regard to sensitivity, area under the curve, and positive predictive value (PPV). Sensitivity ranged from 34% for single-phase planar imaging to 73% for dual-phase studies including an early SPECT/CT scan. The PPV was as high as 86%–91% for dual-phase studies including an early SPECT/CT scan. The specificity was greater than 98% for all of the imaging techniques, and the negative predictive value was greater than 95%. Furthermore, early SPECT/CT had a higher sensitivity and a significantly higher PPV than delayed SPECT/CT. The authors therefore concluded that CT coregistration is a valuable tool for the precise delineation of parathyroid adenomas (Fig. 5).

Superior localization of parathyroid adenomas was also reported by Harris et al. (46). For a series of 23 patients, SPECT/CT performed well for the detection and localization of solitary adenomas (89%), but performance for the detection of multifocal disease was reduced. In a pilot study, Ruf et al. performed low-dose CT for attenuation correction and reported that the sensitivity of attenuation-corrected  $^{99\text{m}}\text{Tc}$ -MIBI SPECT/CT was only slightly higher than that of non-attenuation-corrected SPECT (47). Also, Gayed et al. reported that SPECT/CT was only of limited value (8% of patients) (48). On the contrary, a retrospective study indicated a change in therapeutic management for 39% of patients (14/36) because of the localization of ectopic parathyroid adenomas or accurate localization in patients with distorted neck anatomy (49). Because of some inconsistent reports, a definite role of SPECT/CT in the imaging of parathyroid adenomas has not yet been indicated, and evaluations with larger patient cohorts are needed.

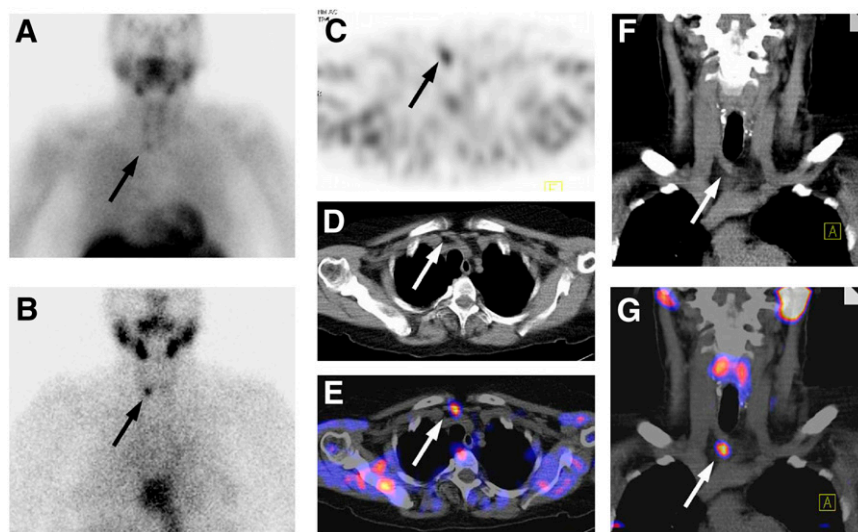


**FIGURE 5.** Parathyroid scintigraphy with SPECT/CT. (A and B) Planar views of  $^{99\text{m}}\text{Tc}$ -MIBI scintigraphy 60 min (A) and 15 min (B) after  $^{99\text{m}}\text{Tc}$ -MIBI injection. Arrows indicate lesions. (C) Transverse section of  $^{99\text{m}}\text{Tc}$ -MIBI SPECT showing mildly intense focal lesion in right lower neck region (arrow). (D and E) Corresponding CT section (D) and fused image (E) indicating parathyroid adenoma below right thyroid gland (arrows). (F and G) Demonstration of parathyroid adenoma (arrows) in corresponding coronal CT (F) and SPECT/CT (G) images.

## SPECT/CT IN TUMORS OF SYMPATHETIC NERVOUS SYSTEM AND ADRENOCORTICAL TUMORS

Morphologic imaging modalities, such as CT or MRI, offer high sensitivity for the detection of tumors of the sympathetic nervous system. The major advantages of radionuclide imaging, such as  $^{123}\text{I}$ -metaiodobenzylguanidine (MIBG) SPECT,  $^{18}\text{F}$ -L-3,4-dihydroxyphenylalanine PET, or  $^{11}\text{C}$ -metahydroxyephedrine (HED) PET, are high specificity, which can be used to better characterize lesions, and superior differentiation of scar tissue and residual tumor after surgery (Fig. 6) (50,51). Radionuclide imaging is also helpful for the detection of extraadrenal tumor sites. In a prospective study, Franzius et al. evaluated the clinical use of  $^{123}\text{I}$ -MIBG SPECT/CT in 19 patients with a variety of tumors of the sympathetic nervous system, including neuroblastoma and pheochromocytoma (52).  $^{123}\text{I}$ -MIBG SPECT/CT had a sensitivity (93%) similar to that (99%) achieved by PET/CT with  $^{11}\text{C}$ -HED as a tracer.  $^{11}\text{C}$ -HED PET/CT was demonstrated to show a higher spatial resolution and to return a final diagnosis within 30 min. SPECT/CT was compromised by a longer examination time and the need for delayed imaging (24 h after tracer administration). However, no superiority of PET/CT over SPECT/CT was observed. Because of the high cost and low availability of  $^{11}\text{C}$ ,  $^{123}\text{I}$ -MIBG SPECT/CT seems to be appropriate for the imaging of tumors derived from the sympathetic nervous system, such as neuroblastoma, pheochromocytoma, ganglioneuroblastoma, and paraganglioma.

Scintigraphic techniques also complement anatomically based imaging modalities for the evaluation of adrenocortical disease. The impact of hybrid SPECT/CT on the performance of functional imaging, such as  $^{75}\text{Se}$ -selenomethylnorcholesterol or  $^{131}\text{I}$ -iodocholesterol imaging, remains to be determined, because only scant data can be found in the literature.

In a pilot study, Even-Sapir et al. reported a change in clinical management for a few patients undergoing  $^{75}\text{Se}$ -cholesterol SPECT/CT (53). Despite an obvious lack of clinical studies demonstrating the superiority of SPECT/CT over separately performed imaging modalities, it can be speculated that hybrid imaging will increase diagnostic accuracy and may lead to the more frequent use of functional imaging techniques.

## SPECT/CT IN NEUROENDOCRINE TUMORS

Neuroendocrine tumors usually exhibit increased expression of somatostatin receptors (SSTR), enabling their detection through the specific binding of radiolabeled ligands, such as  $^{111}\text{In}$ -octreotide or  $^{111}\text{In}$ -pentetretotide. SSTR scintigraphy is predominantly used for the detection of primary tumors or hepatic or mesenteric metastases but can also be used for assessment of the response to treatment with somatostatin analogs. The number of publications illustrating the added value of CT coregistration for SSTR planar imaging or SSTR SPECT is limited. The largest study to date evaluated SSTR SPECT/CT in 72 patients with various neuroendocrine tumors, including 45 carcinoid tumors, medullary thyroid carcinoma, or islet cell tumors (54). No additional information beyond that provided by planar imaging or SPECT was achieved for 48 patients, whereas SPECT/CT improved the localization of scintigraphic findings for 23 patients (32%) and changed clinical management for 14% of patients. For a series of 27 patients with various neuroendocrine tumors, Even-Sapir et al. demonstrated increased accuracy of detection of lesions by  $^{131}\text{I}$ ,  $^{123}\text{I}$ -MIBG,  $^{75}\text{Se}$ -cholesterol, or  $^{111}\text{In}$ -pentetretotide SPECT/CT (53). For one third of patients, a change in clinical

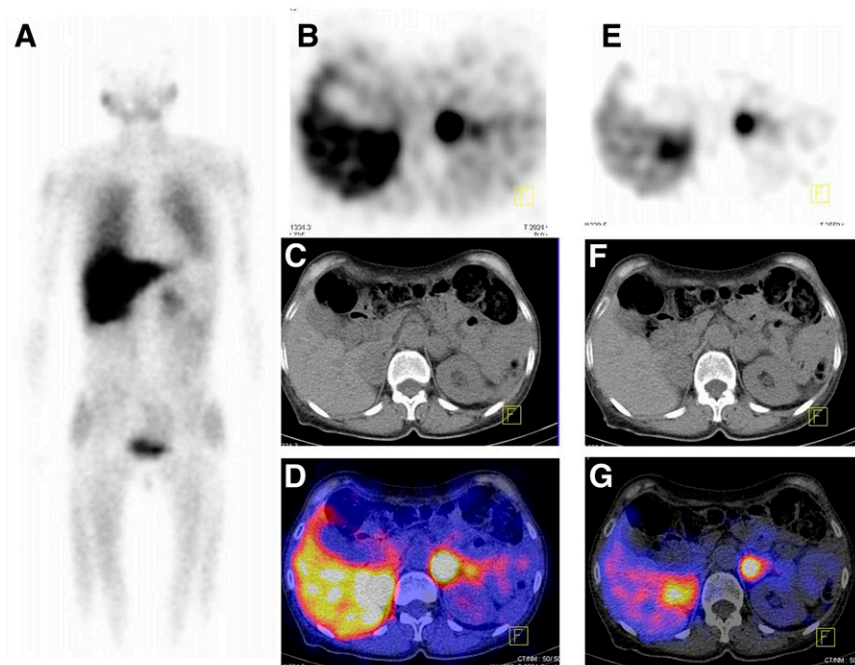


**FIGURE 6.** Diagnosis of pheochromocytoma with  $^{99\text{m}}\text{Tc}$ -MIBG SPECT/CT. (A) Planar image showing mildly intense focal lesion extending to left suprarenal area. (B–D) Corresponding sections of SPECT (B), CT (C), and fused SPECT/CT (D) images showing focal uptake extending to enlarged left adrenal gland, indicating pheochromocytoma. (E–G) Corresponding transverse sections of right adrenal gland showing additional hot spot and enlargement of gland, indicating second pheochromocytoma, which was proven histologically. Lesion may be missed on planar image (A) or overexposed transaxial SPECT image (B).

management occurred. A significant impact of SPECT/CT on therapeutic management was also demonstrated by Hillel et al. for 29 patients with carcinoid or other neuroendocrine tumors (55). The addition of clinically relevant information for 40% of patients by SPECT/CT compared with SPECT was described by Gabriel et al. (56).

### **SPECT/CT IN CARDIAC IMAGING**

As an example of the increased interest in hybrid cardiac imaging, the Society of Nuclear Medicine awarded its 2006 image of the year award to a cardiac SPECT/CT study (57). This study demonstrated a defect in the inferior myocardium together with corresponding stenosis on CT angiography (CTA). Combining function and morphology is highly attractive for several reasons: improved diagnosis and logistics as well as illustrative visualization. In this review, we focus on the methodologic perspective for hybrid SPECT/CT in nuclear perfusion imaging (Table 2), because the number of clinical procedures and research studies is still small compared with the number of studies of conventional methods. Where SPECT, CT, and SPECT/CT are positioned best in the clinical decision-making process is outside the scope of this review; discussion of this topic is ongoing and is the focus of recent reviews (58–60). Specifically, Berman et al. proposed “possible risk-based strategies through which imaging might be used to identify candidates for more intense prevention and risk factor modification strategies as well as those who would benefit from coronary angiography and revascularization” (59). We are convinced that cardiac SPECT/CT will play a prominent role in these scenarios and have compiled arguments ranging from improved attenuation correction to the assessment of complementary information with the potential of reducing radiation burden.

#### **Use of CT for Attenuation Correction**

Nonhomogeneous photon attenuation in the thorax is one of the most notable limitations of myocardial perfusion imaging. It creates the appearance of a nonuniform, regional perfusion distribution even for normal hearts, thus limiting clinical specificity. To overcome this obstacle, the correction of photon attenuation requires the assessment of attenuating tissue in the volume of interest (Fig. 1). Unfortunately, cardiac imaging poses a particular problem for attenuation correction because of respiratory and cardiac motion. Technically, SPECT attenuation correction with external sources was introduced in the early 1990s; retrospectively, however, its success appears to be rather limited. Thus, the integration of CT components in 2000 was a major step forward, with clinically relevant results being reported in larger studies (61,62).

The technical developments were summarized in recent review articles (3,63). Two different technical approaches were previously investigated. The first was a protocol with a radiation burden as low as possible (<0.5 mSv). The second was a CT examination allowing diagnostic imaging that, for cardiac imaging, would be either an assessment of coronary

calcifications or, if the CT system were suitable, contrast-based angiography (typically 1–3 mSv for calcium scoring or 4–14 mSv for CTA). It is important to note that the actual doses varied substantially for the imaging hardware and the imaging protocol used and recently showed a trend toward a decrease, at least for CTA studies. For the low-dose approach and the coronary calcification scan, the contribution to the overall dose is moderate; for SPECT and CTA, the contributions are almost the same (Table 2).

PET/CT studies have already shown that very low-dose CT acquisitions are feasible for attenuation correction (64). Koepfli et al. (65) and a recent study with SPECT/CT confirmed these findings (66). However, a potential misalignment between emission and transmission data poses the risk of incomplete correction and thus artificial perfusion defects and requires careful quality control to avoid reconstruction artifacts. PET/CT (67,68) and SPECT/CT (69,70) studies have shown that the frequency of misalignment is high ( $\leq 50\%$ ) and that the consequences are clinically significant. Fortunately, a recent study with a digital phantom showed that the effects of misalignment are less severe for SPECT/CT than for PET/CT, mainly because of reduced spatial resolution (71). The alignment of SPECT and CT is usually performed manually, a process that contributes to certain variabilities. However, automated approaches for quality control are under investigation (10,72,73). It is relevant that even low-quality CT scans for attenuation correction provide clinically useful information. Goetze et al. reported that for 10% of 200 patients, noncardiac-related abnormal findings were detected (69,70). Similar data with even higher incidence rates are available from cardiac CT studies (74,75). Incidental findings may result in legal liabilities. It is clear that modifications in the clinical reading process are needed.

#### **Cardiac SPECT Versus PET and Absolute Quantification**

The superiority of cardiac PET over cardiac SPECT was demonstrated in several publications (3,58,71,76,77). However, in almost all of these reports, non-attenuation-corrected SPECT was used. Thus, assuming the availability of reliable CT-based attenuation correction for single-photon imaging and given an increased tolerance of motion artifacts, new studies should provide further insight into whether PET will remain superior. From a technical point of view, the capability of PET for absolute quantification in general and for blood flow quantification in particular is a substantial advantage. Nevertheless, through the use of animal models and a SPECT/CT system, it was shown that absolute activity values can be generated when attenuation correction and partial-volume effects are considered (78,79). For assessing absolute flow and coronary flow reserve, imaging with SPECT appears to be promising but requires large-scale validation work (80–82).

#### **Integration of Calcium Scoring CT**

In general, a trend toward the integration of low- and medium-quality CT systems—as opposed to high-end sys-

tems suitable for contrast-enhanced CT of the coronary arteries—into SPECT/CT devices has been observed. Consequently, those hybrid systems are not necessarily suitable for analysis of the vessel lumen with contrast agents but may be capable of the technically less demanding imaging of coronary calcium as a potential marker of atherosclerosis; however, this hypothesis has been debated in the last few years. It is not the aim of this review to repeat this discussion, but some selected, potential hybrid applications deserve mention.

A recent study investigated the incidence of significant calcifications in 84 patients referred for  $^{82}\text{Rb}$  PET with adenosine stress (83). Non-contrast-enhanced CT was used for attenuation correction. Thirty-four patients with negative calcium findings also had normal PET results (negative predictive value, 100%). The remaining 50 patients had calcifications, and a myocardial perfusion defect was detected in 13 patients (PPV, 26%; sensitivity, 100%; specificity, 48%). Using this combined approach, the investigators concluded that myocardial perfusion PET could have been obviated in 63% of patients with no smoking history and no prior myocardial infarction or coronary revascularization procedure and in 37% of the total patient cohort. Although this study was a PET/CT study, this approach might allow a nuclear scan in a resting state to be avoided, and the overall radiation dose from SPECT/CT could be markedly reduced. Similarly, Henneman et al. investigated the hypoenhancement resulting from delayed contrast agent washin in CTA studies (84). On the basis of the fact that the scar scores calculated from SPECT myocardial perfusion imaging and by CTA washin analysis corresponded well for SPECT and CTA, another approach to avoiding a resting SPECT examination could be envisioned. However, although these studies appear to be promising, the incremental value of assessing coronary calcifications or coronary morphology as part of a nuclear examination needs to be investigated in large prospective studies, and it is too early to answer the question of optimal work flow.

#### **Myocardial Perfusion and CT Coronary Angiography**

As with combined PET/CT acquisitions of perfusion and coronary morphology (85), visually very attractive displays can be created with SPECT/CT systems (86). In one of the largest studies to date, including 56 patients with a high prevalence of coronary artery disease, the authors concluded that “hybrid SPECT/CTCA imaging results in improved specificity and PPV to detect hemodynamically significant coronary lesions in patients with chest pain” (87). However, this study also showed that the total radiation burden was as high as 41.5 mSv.

It is interesting that the fusion approach is not restricted to integrated devices (88,89). In particular, for CTA studies, the integrated CT component is typically less advanced than stand-alone CT. Thus, the use of external CT is feasible and may even offer a resolution advantage. Technically, SPECT and CT studies must be spatially registered even with hybrid

cameras because of differences in breathing positions (expiration vs. averaged respiratory motion). A relevant additional aspect of cardiac contrast-enhanced CT is the imaging of delayed enhancement, as in MRI. The different washout rates for contrast agents in normal myocardium and damaged myocardium are now widely used in MRI (90) and recently were used in CT (91,92). Thus, delineating scar tissue with low-dose CT after contrast agent injection appears to be feasible.

In summary, the prospects for hybrid cardiac imaging are promising, and new clinical applications are being proposed. Large, prospective, outcome-based studies for proving these concepts are lacking. In addition, economic and biologic aspects must be considered (93,94). However, reliable attenuation correction and the integration of complementary, multimodality information into an attractive display facilitating communication with cardiologists will influence the future development of nuclear cardiac imaging.

#### **SPECT/CT IN NEUROLOGIC AND PSYCHIATRIC DIAGNOSES**

So far, data on the added value of combined SPECT/CT examinations of the brain remain rather limited. However, the diagnostic value of various cerebral SPECT examinations, such as cerebral perfusion or receptor studies, might be increased, to some extent, by additional CT examinations.

In general, individual CT scan-based attenuation correction of brain SPECT data may lead to improved image quality and more accurate data evaluation (Fig. 1). These features may be particularly important for regional data analysis, such as semiquantitative region-of-interest-based image analysis, as regularly applied for the evaluation of imaging studies of presynaptic dopamine transporters with  $^{123}\text{I}$ -2 $\beta$ -carbomethoxy-3 $\beta$ -(4-iodophenyl)tropane (DaTSCAN; GE Healthcare) or postsynaptic dopamine receptors with  $^{123}\text{I}$ -iodobenzamide. These examinations are usually applied for the verification of idiopathic Parkinson's disease, respectively, the differentiation from atypical Parkinson syndromes. In both types of studies, ratios of striatal to background tracer uptake are calculated, and predefined thresholds for striatum-to-background ratios are used for the differentiation of normal uptake and pathologic findings reflecting reduced receptor or transporter density. For attenuation correction of these studies, ellipse-based calculated attenuation correction techniques, such as the procedure described by Chang (95), are usually applied and have been demonstrated to show sufficient reliability. However, it has been shown that attenuation correction based on individual CT scans produces more accurate results (96). In particular, for borderline findings, it is possible that attenuation correction has a significant influence on quantitative assessment and, thus, on the resulting clinical diagnosis. In such cases, individual CT scan-based attenuation correction may lead to a more appropriate diagnosis. In addition to optimized data quality, access to individual coregistered CT data may also improve the standardized definition and

positioning of regions of interest, particularly in datasets with pathologically low uptake (97). However, a systematic analysis is required to assess differences between individually measured and conventionally calculated attenuation corrections, and clarification of whether currently applied thresholds need to be modified is also required.

In addition to individualized attenuation correction, the performance of CT scans simultaneously with SPECT examinations may offer several additional advantages. A recent study examined the additional diagnostic value of the low-dose (CT) component of a combined  $^{99m}\text{Tc}$ -hexamethylpropyleneamine oxime SPECT/CT examination of cerebral perfusion in a large population (98). Interestingly, 25% of the low-dose CT images demonstrated abnormalities such as infarcts, cerebral atrophy, dilated ventricles, basal ganglion calcifications, and other findings, such as subdural hematoma or meningioma. The authors concluded that the CT component of cerebral perfusion SPECT/CT investigations should be routinely reported separately.

Finally, with the advent of modern SPECT/CT hybrid systems containing state-of-the-art CT scanners, it is possible, in principle, to perform high-quality diagnostic CT examinations of the brain in a single session with simultaneous SPECT examinations. This feature may offer opportunities to assess vascular pathologies, such as cerebral ischemia, stroke, or carotid stenosis, and even to diagnose brain death through the examination of cerebral perfusion with  $^{99m}\text{Tc}$ -hexamethylpropyleneamine oxime in combination with CT assessment of vascular abnormalities (CT perfusion imaging, or CTA). The value of this type of combined examinations has not yet been sufficiently assessed and needs to be evaluated in specific clinical trials.

#### COMBINED SPECT/CT FOR OPTIMIZED DOSIMETRY

The complementation of scintigraphic examinations with detailed anatomic information derived from CT offers the possibility of improving organ-specific dosimetry for radiation treatment planning and radionuclide therapy. Dosimetry for treatment planning and for retrospectively ascertaining the absorbed dose delivered during treatment should be regarded as mandatory for all radionuclide therapies, such as radioiodine ( $^{131}\text{I}$ ) treatment of thyroid cancer; radioimmunotherapy of lymphoma with, for example,  $^{90}\text{Y}$ -ibritumomab tiuxetan; or therapy of neuroectodermal tumors, such as pheochromocytoma, neuroblastoma, or paraganglioma, with  $^{131}\text{I}$ -MIBG. Conventionally, dosimetry for radionuclide treatment has been performed mostly by application of a low dose of the therapeutic radionuclide used for imaging or by application of the therapeutic compound labeled with a different radiotracer more suitable for scintigraphy (e.g.,  $^{111}\text{In}$  or  $^{123}\text{I}$ ) followed by tracer uptake measurements in planar scintigrams. However, more accurate dosimetry may require 3-dimensional assessment, proper attenuation correction of the image data, and assessment of organ or target volumes, which can be derived from

simultaneously acquired CT scans. Several studies have already demonstrated that 3-dimensional dosimetry based on anatomic information derived for regional organ volumes or masses from CT leads to superior assessments of regionally applied doses in critical organs (99–103). Integration of the data collected by multimodality imaging into complex calculation models, such as the Monte Carlo simulation, may significantly improve regional dosimetry for the spatial distribution of the absorbed dose (104).

In addition to dosimetry of critical organs at risk, evaluation by multimodality imaging with SPECT/CT may also allow accurate dosimetry of tumor targets for treatment planning and evaluation of the response to radionuclide therapy (105). This process may also be valuable for establishing a clear correlation between the absorbed dose and the biologic effect.

In summary, it appears likely that combined SPECT/CT will be highly useful for performing valid and clinically applicable dosimetry, for improving treatment planning, and for ensuring safe and effective radionuclide therapy.

Furthermore, combined SPECT/CT may also be useful for planning radiation treatment for prostate cancer. Hybrid imaging of capromab pendetide (Prostascint; Cytogen) with SPECT and CT has been demonstrated to show increased sensitivity for the identification of prostate cancer. Recently, it was proposed that this combined imaging approach be used to confine the dose escalation of radiation treatment to discrete regions of known disease, as defined by focal uptake on fused radioimmunoscintigraphic and anatomic image sets (106). It has been suggested that intensification of treatment directed to tumor targets without an increase in rectal toxicity may be achieved. Suggestions also have been extended toward guiding the implantation of radioactive seeds in brachytherapy (107). In general, it may be assumed that SPECT/CT will be equally valid for individualized planning of radiation treatment for other tumor entities, and further clinical research should be encouraged.

#### CONCLUSION

The role of integrated SPECT/CT is growing, especially in oncologic applications. CT coregistration results in higher specificity as well as sensitivity of scintigraphic findings and markedly reduces the number of indeterminate findings. The superiority of SPECT/CT over planar scintigraphy or SPECT has been clearly demonstrated for the imaging of benign and malignant skeletal diseases, thyroid cancer, neuroendocrine cancer, parathyroid adenoma, and mapping of SLNs in the head and neck and in the pelvic region. Studies demonstrating superiority in other clinical applications are lacking; however, pilot studies have encouraged the use of SPECT/CT in cardiac and neurologic imaging. Interesting developments occurring with less frequently used radiopharmaceuticals and imaging technologies may become clinically relevant in the near future.

## REFERENCES

- Czermin J, Allen-Auerbach M, Schelbert HR. Improvements in cancer staging with PET/CT: literature-based evidence as of September 2006. *J Nucl Med*. 2007;48(suppl 1):78S–88S.
- von Schultheiss GK, Steinert HC, Hany TF. Integrated PET/CT: current applications and future directions. *Radiology*. 2006;238:405–422.
- O'Connor MK, Kemp BJ. Single-photon emission computed tomography/computed tomography: basic instrumentation and innovations. *Semin Nucl Med*. 2006;36:258–266.
- Perault C, Schwartz C, Wampach H, Liehn JC, Delisle MJ. Thoracic and abdominal SPECT-CT image fusion without external markers in endocrine carcinomas. The Group of Thyroid Tumoral Pathology of Champagne-Ardenne. *J Nucl Med*. 1997;38:1234–1242.
- Frank A, Lefkowitz D, Jaeger S, et al. Decision logic for retreatment of asymptomatic lung cancer recurrence based on positron emission tomography findings. *Int J Radiat Oncol Biol Phys*. 1995;32:1495–1512.
- Forster GJ, Laumann C, Nickel O, Kann P, Rieker O, Bartenstein P. SPET/CT image co-registration in the abdomen with a simple and cost-effective tool. *Eur J Nucl Med Mol Imaging*. 2003;30:32–39.
- Hasegawa BH, Wong KH, Iwata K, et al. Dual-modality imaging of cancer with SPECT/CT. *Technol Cancer Res Treat*. 2002;1:449–458.
- Bocher M, Balan A, Krausz Y, et al. Gamma camera-mounted anatomical X-ray tomography: technology, system characteristics and first images. *Eur J Nucl Med*. 2000;27:619–627.
- Xia W, Lewitt RM, Edholm PR. Fourier correction for spatially variant collimator blurring in SPECT. *IEEE Trans Med Imaging*. 1995;14:100–115.
- Chen J, Caputlu-Wilson SF, Shi H, Galt JR, Faber TL, Garcia EV. Automated quality control of emission-transmission misalignment for attenuation correction in myocardial perfusion imaging with SPECT-CT systems. *J Nucl Cardiol*. 2006;13:43–49.
- Kuehl H, Veit P, Rosenbaum SJ, Bockisch A, Antoch G. Can PET/CT replace separate diagnostic CT for cancer imaging? Optimizing CT protocols for imaging cancers of the chest and abdomen. *J Nucl Med*. 2007;48(suppl 1):45S–57S.
- Even-Sapir E, Lerman H, Lievshitz G, et al. Lymphoscintigraphy for sentinel node mapping using a hybrid SPECT/CT system. *J Nucl Med*. 2003;44:1413–1420.
- Zhang WJ, Zheng R, Wu LY, Li XG, Li B, Chen SZ. Clinical application of sentinel lymph node detection to early stage cervical cancer [in Chinese]. *Ai Zheng*. 2006;25:224–228.
- Sherif A, Garske U, de la Torre M, Thorn M. Hybrid SPECT-CT: an additional technique for sentinel node detection of patients with invasive bladder cancer. *Eur Urol*. 2006;50:83–91.
- Khafif A, Schneebaum S, Fliss DM, et al. Lymphoscintigraphy for sentinel node mapping using a hybrid single photon emission CT (SPECT)/CT system in oral cavity squamous cell carcinoma. *Head Neck*. 2006;28:874–879.
- Bilde A, Von Buchwald C, Mortensen J, et al. The role of SPECT-CT in the lymphoscintigraphic identification of sentinel nodes in patients with oral cancer. *Acta Otolaryngol*. 2006;126:1096–1103.
- Keski-Santti H, Matzke S, Kauppinen T, Tornwall J, Atula T. Sentinel lymph node mapping using SPECT-CT fusion imaging in patients with oral cavity squamous cell carcinoma. *Eur Arch Otorhinolaryngol*. 2006;263:1008–1012.
- Wagner A, Schicho K, Glaser C, et al. SPECT-CT for topographic mapping of sentinel lymph nodes prior to gamma probe-guided biopsy in head and neck squamous cell carcinoma. *J Craniomaxillofac Surg*. 2004;32:343–349.
- Husarik DB, Steinert HC. Single-photon emission computed tomography/computed tomography for sentinel node mapping in breast cancer. *Semin Nucl Med*. 2007;37:29–33.
- Lerman H, Metzger U, Lievshitz G, Sperber F, Shneebaum S, Even-Sapir E. Lymphoscintigraphic sentinel node identification in patients with breast cancer: the role of SPECT-CT. *Eur J Nucl Med Mol Imaging*. 2006;33:329–337.
- Gallowitsch HJ, Kraschl P, Igerc I, et al. Sentinel node SPECT-CT in breast cancer: can we expect any additional and clinically relevant information? *Nuklearmedizin*. 2007;46:252–256.
- van der Ploeg IM, Valdes Olmos RA, Nieweg OE, Rutgers EJ, Kroon BB, Hoefnagel CA. The additional value of SPECT/CT in lymphatic mapping in breast cancer and melanoma. *J Nucl Med*. 2007;48:1756–1760.
- Lerman H, Lievshitz G, Zak O, Metzger U, Schneebaum S, Even-Sapir E. Improved sentinel node identification by SPECT/CT in overweight patients with breast cancer. *J Nucl Med*. 2007;48:201–206.
- Hamaoka T, Madewell JE, Podoloff DA, Hortobagyi GN, Ueno NT. Bone imaging in metastatic breast cancer. *J Clin Oncol*. 2004;22:2942–2953.
- Minoves M. Bone and joint sports injuries: the role of bone scintigraphy. *Nucl Med Commun*. 2003;24:3–10.
- Even-Sapir E. Imaging of malignant bone involvement by morphologic, scintigraphic, and hybrid modalities. *J Nucl Med*. 2005;46:1356–1367.
- Römer W, Nomayr A, Uder M, Bautz W, Kuwert T. SPECT-guided CT for evaluating foci of increased bone metabolism classified as indeterminate on SPECT in cancer patients. *J Nucl Med*. 2006;47:1102–1106.
- Seo Y, Wong KH, Sun M, Franc BL, Hawkins RA, Hasegawa BH. Correction of photon attenuation and collimator response for a body-contouring SPECT/CT imaging system. *J Nucl Med*. 2005;46:868–877.
- Römer W, Reichel N, Vija HA, et al. Isotropic reconstruction of SPECT data using OSEM3D: correlation with CT. *Acad Radiol*. 2006;13:496–502.
- Horger M, Eschmann SM, Pfannenbergs C, et al. Evaluation of combined transmission and emission tomography for classification of skeletal lesions. *AJR*. 2004;183:655–661.
- Utsunomiya D, Shiraishi S, Imuta M, et al. Added value of SPECT/CT fusion in assessing suspected bone metastasis: comparison with scintigraphy alone and nonfused scintigraphy and CT. *Radiology*. 2006;238:264–271.
- Even-Sapir E, Flusser G, Lerman H, Lievshitz G, Metzger U. SPECT/multislice low-dose CT: a clinically relevant constituent in the imaging algorithm of nononcologic patients referred for bone scintigraphy. *J Nucl Med*. 2007;48:319–324.
- Bar-Shalom R, Yefremov N, Guralnik L, et al. SPECT/CT using  $^{67}\text{Ga}$  and  $^{111}\text{In}$ -labeled leukocyte scintigraphy for diagnosis of infection. *J Nucl Med*. 2006;47:587–594.
- Filippi L, Schillaci O. Usefulness of hybrid SPECT/CT in  $^{99\text{m}}\text{Tc}$ -HMPAO-labeled leukocyte scintigraphy for bone and joint infections. *J Nucl Med*. 2006;47:1908–1913.
- Horger M, Eschmann SM, Pfannenbergs C, et al. Added value of SPECT/CT in patients suspected of having bone infection: preliminary results. *Arch Orthop Trauma Surg*. 2007;127:211–221.
- Ingui CJ, Shah NP, Oates ME. Infection scintigraphy: added value of single-photon emission computed tomography/computed tomography fusion compared with traditional analysis. *J Comput Assist Tomogr*. 2007;31:375–380.
- Nathan J, Crawford JA, Sodde DB, Bakale G. Fused SPECT/CT imaging of peri-iliopsoas infection using indium-111-labeled leukocytes. *Clin Nucl Med*. 2006;31:801–802.
- Palestro CJ, Love C, Miller TT. Diagnostic imaging tests and microbial infections. *Cell Microbiol*. 2007;9:2323–2333.
- Roach PJ, Schembri GP, Ho Shon IA, Bailey EA, Bailey DL. SPECT/CT imaging using a spiral CT scanner for anatomical localization: impact on diagnostic accuracy and reporter confidence in clinical practice. *Nucl Med Commun*. 2006;27:977–987.
- Slart RH, Koopmans KP, Gunneweg P, Luijckx GJ, de Jong BM. Persistent aseptic meningitis due to post-surgical spinal CSF leakage: value of fused  $^{111\text{m}}\text{In}$ -DTPA SPECT-CT cisternography. *Eur J Nucl Med Mol Imaging*. 2006;33:856.
- Ingui CJ, Shah NP, Oates ME. Endocrine neoplasm scintigraphy: added value of fusing SPECT/CT images compared with traditional side-by-side analysis. *Clin Nucl Med*. 2006;31:665–672.
- Tharp K, Israel O, Hausmann J, et al. Impact of  $^{131}\text{I}$ -SPECT/CT images obtained with an integrated system in the follow-up of patients with thyroid carcinoma. *Eur J Nucl Med Mol Imaging*. 2004;31:1435–1442.
- Yamamoto Y, Nishiyama Y, Monden T, Matsumura Y, Satoh K, Ohkawa M. Clinical usefulness of fusion of  $^{131}\text{I}$  SPECT and CT images in patients with differentiated thyroid carcinoma. *J Nucl Med*. 2003;44:1905–1910.
- Ruf J, Lehmkuhl L, Bertram H, et al. Impact of SPECT and integrated low-dose CT after radioiodine therapy on the management of patients with thyroid carcinoma. *Nucl Med Commun*. 2004;25:1177–1182.
- Lavelly WC, Goetze S, Friedman KP, et al. Comparison of SPECT/CT, SPECT, and planar imaging with single- and dual-phase  $^{99\text{m}}\text{Tc}$ -sestamibi parathyroid scintigraphy. *J Nucl Med*. 2007;48:1084–1089.
- Harris L, Yoo J, Driedger A, et al. Accuracy of technetium-99m SPECT-CT hybrid images in predicting the precise intraoperative anatomical location of parathyroid adenomas. *Head Neck*. 2008;30:509–517.
- Ruf J, Seehofer D, Denecke T, et al. Impact of image fusion and attenuation correction by SPECT-CT on the scintigraphic detection of parathyroid adenomas. *Nuklearmedizin*. 2007;46:15–21.
- Gayed IW, Kim EE, Broussard WF, et al. The value of  $^{99\text{m}}\text{Tc}$ -sestamibi SPECT/CT over conventional SPECT in the evaluation of parathyroid adenomas or hyperplasia. *J Nucl Med*. 2005;46:248–252.
- Krausz Y, Bettman L, Guralnik L, et al. Technetium-99m-MIBI SPECT/CT in primary hyperparathyroidism. *World J Surg*. 2006;30:76–83.
- Avram AM, Fig LM, Gross MD. Adrenal gland scintigraphy. *Semin Nucl Med*. 2006;36:212–227.

51. Gross MD, Avram A, Fig LM, Rubello D. Contemporary adrenal scintigraphy. *Eur J Nucl Med Mol Imaging*. 2007;34:547-557.
52. Franzius C, Hermann K, Weckesser M, et al. Whole-body PET/CT with <sup>11</sup>C-meta-hydroxyephedrine in tumors of the sympathetic nervous system: feasibility study and comparison with <sup>123</sup>I-MIBG SPECT/CT. *J Nucl Med*. 2006;47:1635-1642.
53. Even-Sapir E, Keidar Z, Sachs J, et al. The new technology of combined transmission and emission tomography in evaluation of endocrine neoplasms. *J Nucl Med*. 2001;42:998-1004.
54. Krausz Y, Keidar Z, Kogan I, et al. SPECT/CT hybrid imaging with <sup>111</sup>In-pentetreotide in assessment of neuroendocrine tumours. *Clin Endocrinol (Oxf)*. 2003;59:565-573.
55. Hillel PG, van Beek EJ, Taylor C, et al. The clinical impact of a combined gamma camera/CT imaging system on somatostatin receptor imaging of neuroendocrine tumours. *Clin Radiol*. 2006;61:579-587.
56. Gabriel M, Hausler F, Bale R, et al. Image fusion analysis of <sup>99m</sup>Tc-HYNIC-Tyr(3)-octreotide SPECT and diagnostic CT using an immobilisation device with external markers in patients with endocrine tumours. *Eur J Nucl Med Mol Imaging*. 2005;32:1440-1451.
57. 2006 Image of the year: focus on cardiac SPECT/CT. *J Nucl Med*. 2006;47:14N-15N.
58. Berman DS, Hachamovitch R, Shaw LJ, et al. Roles of nuclear cardiology, cardiac computed tomography, and cardiac magnetic resonance: assessment of patients with suspected coronary artery disease. *J Nucl Med*. 2006;47:74-82.
59. Berman DS, Shaw LJ, Hachamovitch R, et al. Comparative use of radionuclide stress testing, coronary artery calcium scanning, and noninvasive coronary angiography for diagnostic and prognostic cardiac assessment. *Semin Nucl Med*. 2007;37:2-16.
60. Raggi P, Berman DS. Computed tomography coronary calcium screening and myocardial perfusion imaging. *J Nucl Cardiol*. 2005;12:96-103.
61. Dondi M, Fagioli G, Salgarello M, Zoboli S, Nanni C, Cidda C. Myocardial SPECT: what do we gain from attenuation correction (and when)? *Q J Nucl Med Mol Imaging*. 2004;48:181-187.
62. Masood Y, Liu YH, Depuey G, et al. Clinical validation of SPECT attenuation correction using x-ray computed tomography-derived attenuation maps: multicenter clinical trial with angiographic correlation. *J Nucl Cardiol*. 2005;12:676-686.
63. Madsen MT. Recent advances in SPECT imaging. *J Nucl Med*. 2007;48:661-673.
64. Souvatzoglou M, Bengel F, Busch R, et al. Attenuation correction in cardiac PET/CT with three different CT protocols: a comparison with conventional PET. *Eur J Nucl Med Mol Imaging*. 2007;34:1991-2000.
65. Koepfli P, Hany TF, Wyss CA, et al. CT attenuation correction for myocardial perfusion quantification using a PET/CT hybrid scanner. *J Nucl Med*. 2004;45:537-542.
66. Preuss R, Weise R, Lindner O, Fricke E, Fricke H, Burchert W. Optimisation of protocol for low dose CT-derived attenuation correction in myocardial perfusion SPECT imaging. *Eur J Nucl Med Mol Imaging*. 2008;35:1133-1141.
67. Martinez-Moller A, Souvatzoglou M, Navab N, Schwaiger M, Nekolla SG. Artifacts from misaligned CT in cardiac perfusion PET/CT studies: frequency, effects, and potential solutions. *J Nucl Med*. 2007;48:188-193.
68. Gould KL, Pan T, Loghini C, Johnson NP, Guha A, Sdringola S. Frequent diagnostic errors in cardiac PET/CT due to misregistration of CT attenuation and emission PET images: a definitive analysis of causes, consequences, and corrections. *J Nucl Med*. 2007;48:1112-1121.
69. Goetze S, Brown TL, Lavelly WC, Zhang Z, Bengel FM. Attenuation correction in myocardial perfusion SPECT/CT: effects of misregistration and value of reregistration. *J Nucl Med*. 2007;48:1090-1095.
70. Goetze S, Wahl RL. Prevalence of misregistration between SPECT and CT for attenuation-corrected myocardial perfusion SPECT. *J Nucl Cardiol*. 2007;14:200-206.
71. McQuaid SJ, Hutton BF. Sources of attenuation-correction artefacts in cardiac PET/CT and SPECT/CT. *Eur J Nucl Med Mol Imaging*. 2008;35:1117-1123.
72. Guetter C, Wacker M, Xu C, Hornegger J. Registration of cardiac SPECT/CT data through weighted intensity co-occurrence priors. *Med Image Comput Assist Interv Int Conf Med Image Comput Assist Interv*. 2007;10:725-733.
73. Kovalski G, Israel O, Keidar Z, Frenkel A, Sachs J, Azhari H. Correction of heart motion due to respiration in clinical myocardial perfusion SPECT scans using respiratory gating. *J Nucl Med*. 2007;48:630-636.
74. Onuma Y, Tanabe K, Nakazawa G, et al. Noncardiac findings in cardiac imaging with multidetector computed tomography. *J Am Coll Cardiol*. 2006;48:402-406.
75. Schietinger BJ, Bozlar U, Hagspiel KD, et al. The prevalence of extracardiac findings by multidetector computed tomography before atrial fibrillation ablation. *Am Heart J*. 2008;155:254-259.
76. Ballok ZE. Nuclear cardiology. *Heart Lung Circ*. 2005;14(suppl 2):S27-S30.
77. Slomka PJ, Berman DS, Germano G. Applications and software techniques for integrated cardiac multimodality imaging. *Expert Rev Cardiovasc Ther*. 2008;6:27-41.
78. Kalki K, Blankespoor SC, Brown JK, et al. Myocardial perfusion imaging with a combined x-ray CT and SPECT system. *J Nucl Med*. 1997;38:1535-1540.
79. Da Silva AJ, Tang HR, Wong KH, Wu MC, Dae MW, Hasegawa BH. Absolute quantification of regional myocardial uptake of <sup>99m</sup>Tc-sestamibi with SPECT: experimental validation in a porcine model. *J Nucl Med*. 2001;42:772-779.
80. Storto G, Sorrentino AR, Pellegrino T, Liuzzi R, Petretta M, Cuocolo A. Assessment of coronary flow reserve by sestamibi imaging in patients with typical chest pain and normal coronary arteries. *Eur J Nucl Med Mol Imaging*. 2007;34:1156-1161.
81. Storto G, Cirillo P, Vicario ML, et al. Estimation of coronary flow reserve by Tc-99m sestamibi imaging in patients with coronary artery disease: comparison with the results of intracoronary Doppler technique. *J Nucl Cardiol*. 2004;11:682-688.
82. Lodge MA, Bengel FM. Methodology for quantifying absolute myocardial perfusion with PET and SPECT. *Curr Cardiol Rep*. 2007;9:121-128.
83. Esteves FP, Sanyal R, Santana CA, Shaw L, Raggi P. Potential impact of noncontrast computed tomography as gatekeeper for myocardial perfusion positron emission tomography in patients admitted to the chest pain unit. *Am J Cardiol*. 2008;101:149-152.
84. Henneman MM, Schuijff JD, Dibbets-Schneider P, et al. Comparison of multislice computed tomography to gated single-photon emission computed tomography for imaging of healed myocardial infarcts. *Am J Cardiol*. 2008;101:144-148.
85. Namdar M, Hany TF, Koepfli P, et al. Integrated PET/CT for the assessment of coronary artery disease: a feasibility study. *J Nucl Med*. 2005;46:930-935.
86. Ghersin E, Keidar Z, Rispler S, et al. Images in cardiovascular medicine: hybrid cardiac single photon emission computed tomography/computed tomography imaging with myocardial perfusion single photon emission computed tomography and multidetector computed tomography coronary angiography for the assessment of unstable angina pectoris after coronary artery bypass grafting. *Circulation*. 2006;114:e237-e239.
87. Rispler S, Keidar Z, Ghersin E, et al. Integrated single-photon emission computed tomography and computed tomography coronary angiography for the assessment of hemodynamically significant coronary artery lesions. *J Am Coll Cardiol*. 2007;49:1059-1067.
88. Gaemperli O, Schepis T, Kalf V, et al. Validation of a new cardiac image fusion software for three-dimensional integration of myocardial perfusion SPECT and stand-alone 64-slice CT angiography. *Eur J Nucl Med Mol Imaging*. 2007;34:1097-1106.
89. Gaemperli O, Schepis T, Valenta I, et al. Cardiac image fusion from stand-alone SPECT and CT: clinical experience. *J Nucl Med*. 2007;48:696-703.
90. Kim RJ, Fieno DS, Parrish TB, et al. Relationship of MRI delayed contrast enhancement to irreversible injury, infarct age, and contractile function. *Circulation*. 1999;100:1992-2002.
91. Mahnken AH, Koos R, Katoh M, et al. Sixteen-slice spiral CT versus MR imaging for the assessment of left ventricular function in acute myocardial infarction. *Eur Radiol*. 2005;15:714-720.
92. Lardo AC, Cordeiro MA, Silva C, et al. Contrast-enhanced multidetector computed tomography viability imaging after myocardial infarction: characterization of myocyte death, microvascular obstruction, and chronic scar. *Circulation*. 2006;113:394-404.
93. Picano E. Economic and biological costs of cardiac imaging. *Cardiovasc Ultrasound*. 2005;3:13.
94. Wijns W. Anatomic-functional imaging by single-photon emission computed tomography/computed tomography as the cornerstone of diagnosis and treatment for coronary patients: a glimpse into the (near) future? *J Am Coll Cardiol*. 2007;49:1068-1070.
95. Chang L. A method for attenuation correction in radio-nuclide computed tomography. *IEEE Trans Nucl Sci*. 1978;25:638-643.
96. Hayashi M, Deguchi J, Utsunomiya K, et al. Comparison of methods of attenuation and scatter correction in brain perfusion SPECT. *J Nucl Med Technol*. 2005;33:224-229.
97. Van Laere K, Koole M, D'Asseler Y, et al. Automated stereotactic standardization of brain SPECT receptor data using single-photon transmission images. *J Nucl Med*. 2001;42:361-375.

98. Sulkin TV, Cousens C. SPECTCT cerebral perfusion scintigraphy; is the low-dose CT component of diagnostic value? *Clin Radiol*. 2008;63:289–298.
99. Boucek JA, Turner JH. Validation of prospective whole-body bone marrow dosimetry by SPECT/CT multimodality imaging in <sup>131</sup>I-anti-CD20 rituximab radioimmunotherapy of non-Hodgkin's lymphoma. *Eur J Nucl Med Mol Imaging*. 2005;32:458–469.
100. Rajendran JG, Fisher DR, Gopal AK, Durack LD, Press OW, Eary JF. High-dose <sup>131</sup>I-tositumomab (anti-CD20) radioimmunotherapy for non-Hodgkin's lymphoma: adjusting radiation absorbed dose to actual organ volumes. *J Nucl Med*. 2004;45:1059–1064.
101. Thierens HM, Monsieurs MA, Bacher K. Patient dosimetry in radionuclide therapy: the whys and the wherefores. *Nucl Med Commun*. 2005;26:593–599.
102. Cremonesi M, Ferrari M, Grana CM, et al. High-dose radioimmunotherapy with <sup>90</sup>Y-ibritumomab tiuxetan: comparative dosimetric study for tailored treatment. *J Nucl Med*. 2007;48:1871–1879.
103. Assie K, Dieudonne A, Gardin I, Buvat I, Tilly H, Vera P. Comparison between 2D and 3D dosimetry protocols in <sup>90</sup>Y-ibritumomab tiuxetan radioimmunotherapy of patients with non-Hodgkin's lymphoma. *Cancer Biother Radiopharm*. 2008;23:53–64.
104. Prideaux AR, Song H, Hobbs RF, et al. Three-dimensional radiobiologic dosimetry: application of radiobiologic modeling to patient-specific 3-dimensional imaging-based internal dosimetry. *J Nucl Med*. 2007;48:1008–1016.
105. Flux G, Bardies M, Monsieurs M, Savolainen S, Strands SE, Lassmann M. The impact of PET and SPECT on dosimetry for targeted radionuclide therapy. *Z Med Phys*. 2006;16:47–59.
106. Ellis RJ, Kaminsky DA. Fused radioimmunoscinigraphy for treatment planning. *Rev Urol*. 2006;8(suppl 1):S11–S19.
107. Sodee DB, Sodee AE, Bakale G. Synergistic value of single-photon emission computed tomography/computed tomography fusion to radioimmunoscinigraphic imaging of prostate cancer. *Semin Nucl Med*. 2007;37:17–28.